Yafet-Kittel Angles in Zinc-Nickel Ferrites

N. S. SATYA MURTHY, M. G. NATERA,* S. I. YOUSSEF,† AND R. J. BEGUM
Bhabha Atomic Research Centre, Trombay, Bombay-85, India

AND

C. M. SRIVASTAVA
Indian Institute of Technology, Powai, Bombay-85, India

(Received 22 October 1968)

The chemical and magnetic structures of the $Zn_xNi_{1-x}Fe_2O_4$ system have been determined using neutron diffraction for $x=0$, 0.25, 0.50, and 0.75. The data yield a cation distribution $(Zn_x^{2+}Fe_{1-x}^{3+})$ $[Ni_{1-x}^{2+}Fe_{1+x}^{3+}]$. All the mixed ferrites show a noncollinear, Yafet-Kittel (YK) type of magnetic ordering. The YK angles increase with the zinc content and for a given composition decrease with increasing temperature. For $x=0.25$ and 0.50, there is a transition from the YK to Néel type of ordering prior to the paramagnetic transition. The Néel region decreases with increasing x; thus, for $x=0.75$, there is no Néel region, while $NiFe_2O_4$ has the Néel type of ordering at all temperatures. The YK angle can be analytically related to x, using the molecular-field theory. The angles predicted in this manner are consistent with a three-sublattice molecular-field analysis of the paramagnetic susceptibility data of Néel and Brochet.

INTRODUCTION

THE behavior of the saturation magnetization of $Zn_xNi_{1-x}Fe_2O_4$ with respect to zinc content has been determined by various workers.[1–5] To explain this behavior, various theories[1,4,6,7] have been proposed, based on (a) the occupation of the octahedral sites by Zn^{2+} ions, (b) statistical considerations taking into account random incomplete linkages A-O-B, which result when nonmagnetic ions replace magnetic ions in the structure, and (c) the occurrence of noncollinear magnetic structures.

Site-preference calculations,[8,9] neutron-diffraction results on $ZnFe_2O_4$[10] and $Zn_{0.5}Ni_{0.5}Fe_2O_4$,[11] and cation distributions in other spinels containing Zn^{2+} ions[12] show that Zn^{2+} ions invariably occupy the tetrahedral sites, so that explanations based on (a) are not correct. Similarly, theories based on (b) cannot account for Mössbauer-spectra measurements,[13,14] which show the existence of the hyperfine fields at the Fe^{57} nuclei on the A and B sites and for the absence of any pronounced paramagnetic neutron scattering by the ferrites investigated in the present work.

The occurrence of noncollinear spin arrangements in the Zn-Ni system has been suggested by Yafet and Kittel.[7] Recently, Kedem and Rothem[15] suspected $NiFe_2O_4$ itself to have a Yafet-Kittel (YK) type of ordering from their Mössbauer measurements. Their results were, however, contradicted by the Mössbauer results of Chappert and Frankel.[16] Neutron-diffraction studies have previously been made by Hastings and Corliss on $NiFe_2O_4$[10] at room temperature and on $ZnFe_2O_4$[10,17] down to liquid-helium temperatures. The observed diffraction intensities in $NiFe_2O_4$ have been accounted for using the Néel coupling scheme between the spins with the assumption of a composite form factor for the ferrite. For the intermediate composition $Zn_{0.5}Ni_{0.5}Fe_2O_4$, neutron-diffraction work at room temperature and at 330°C was carried out by Wilson and Kasper.[11] They concluded that the magnetic structure is of the Néel type with 60% of the Fe^{3+} ions oriented and all the Ni^{2+} ions completely disordered. This conclusion, however, is not borne out by a corresponding intensity due to paramagnetic scattering in the diffraction pattern. Furthermore, the strong Ni^{2+}-Ni^{2+} superexchange interactions encountered in many compounds containing nickel make it implausible that they are not oriented in the Zn-Ni ferrite system.

In view of these uncertainties, neutron-diffraction studies on the mixed ferrites $Zn_xNi_{1-x}Fe_2O_4$ with $x=0$, 0.25, 0.50, and 0.75 were carried out at various temperatures to determine the cation distributions and the magnetic structures. The sublattice magnetizations and the Néel temperatures have also been determined.

---

* I.A.E.A. Fellow from the Philippine Atomic Research Center Diliman, Quezon City, Philippines.

† Guest Scientist from the U.A.R. Atomic Energy Establishment, Cairo, U.A.R.

[1] E. W. Gorter, Philips Res. Rept. **9**, 321 (1954).

[2] J. Smit and H. P. J. Wijn, *Ferrites* (Wiley-Interscience, Inc., New York, 1959).

[3] R. Pauthenet, Ann. Phys. (N.Y.) **7**, 710 (1952).

[4] E. A. Sobotta and J. Voigtlander, Z. Physik Chem. Neue Folge **39**, 54 (1963).

[5] C. Srinivasan, Ph.D. thesis, Moscow University, 1967 (unpublished).

[6] M. A. Gilleo, J. Phys. Chem. Solids **13**, 33 (1960).

[7] Y. Yafet and C. Kittel, Phys. Rev. **87**, 290 (1952).

[8] A. Miller, J. Appl. Phys. **30**, 248 (1959).

[9] J. B. Goodenough, in *Magnetism*, edited by G. T. Rado and H. Suhl (Academic Press Inc., New York, 1963), Vol. 3.

[10] J. M. Hastings and L. M. Corliss, Rev. Mod. Phys. **25**, 114 (1953).

[11] V. C. Wilson and J. S. Kasper, Phys. Rev. **95**, 1408 (1954).

[12] J. B. Goodenough, *Magnetism and the Chemical Bond* (Wiley-Interscience, Inc., New York, 1963).

[13] V. I. Gol'danskiĭ, V. F. Belov, M. N. Divishera, and V. A. Trukhtanov, Zh. Eksperim. i Teor. Fiz. **49**, 1681 (1965) [English transl.: Soviet Phys.—JETP **22**, 1149 (1966)].

[14] S. C. Bhargava (private communication).

[15] D. Kedem and T. Rothem, Phys. Rev. Letters **18**, 165 (1967).

[16] J. Chappert and R. B. Frankel, Phys. Rev. Letters **19**, 571 (1967).

[17] J. M. Hastings and L. M. Corliss, Phys. Rev. **102**, 1460 (1966).

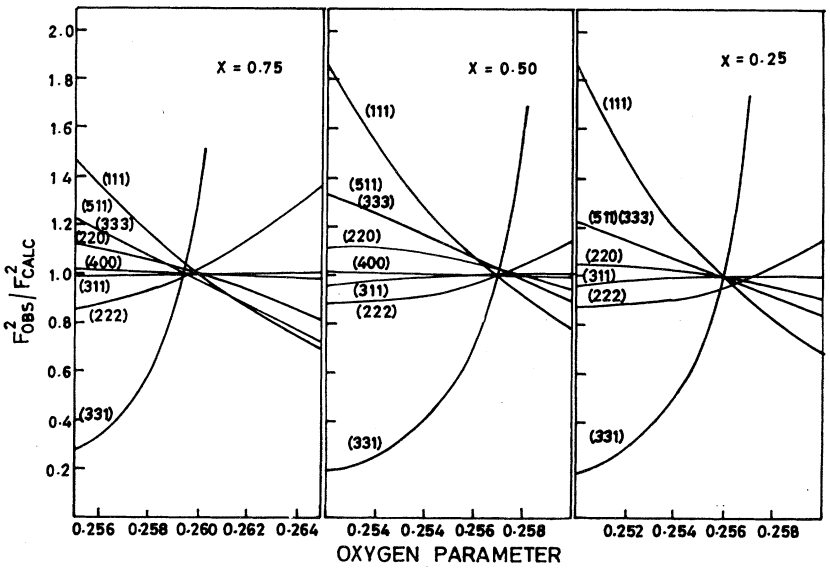

FIG. 1. Dependence of the ratio F_{obs}^2/F_{calc}^2 upon the oxygen parameter for various Bragg reflections for $x=0.25$, 0.50, and 0.75. The intersection of the curves with the line F_{obs}^2/F_{calc}^2 equal to unity yields the value of the oxygen parameter.

From the analysis of the neutron-diffraction data there is definite evidence that the mixed ferrites exhibit a noncollinear arrangement of the YK type while $NiFe_2O_4$ shows a Néel type of ordering. The YK angles (defined in the inset of Fig. 2) increase gradually with increasing zinc content and extrapolate to 90° for $ZnFe_2O_4$. The YK angles have been found to be strongly temperature-dependent, going to zero at temperatures lower than the corresponding Néel temperatures. A Néel type of ordering exists between these two transition temperatures, the region of stability of the Néel configuration decreasing with increasing x.

The occurrence of YK angles can be accounted for on a three-sublattice model in the molecular-field approximation. Using appropriate inter- and intrasublattice molecular-field constants, the YK angles have been found to be consistent with the high-temperature susceptibility data.

EXPERIMENT

The samples were prepared by the usual ceramic sintering process. NiO, ZnO, and Fe_2O_3 were mixed intimately in the stoichiometric proportion and preheated in air at a temperature of 900°C for several hours. The resulting powder was compressed applying a pressure of 1.4 kbar into pellets having 15 mm diam and 3 mm thickness. The pellets were sintered in air at 1250°C for 8 h and furnace-cooled. Chemical analysis showed the desired stoichiometric compositions.

CRYSTAL-STRUCTURE PARAMETERS

X-ray diffractometer traces were obtained using Fe $K\alpha$ radiation to determine precisely the lattice constants. These values (shown in Table I along with other parameters) agree very well with the lattice-constant determination of Sage and Guillaud[18] using Cu $K\alpha$ radiation. For all the ferrites except $NiFe_2O_4$ neutron-diffraction patterns were taken from 100°K to temperatures higher than their respective Néel temperatures. From the intensities of nuclear reflections at room temperature and patterns above the Néel temperatures, the effective A- and B-site scattering amplitudes, oxygen parameter, and Debye temperature were determined. The sublattice magnetizations were determined by following the temperature dependence of appropriate reflections. The graphical method of plotting the ratios of observed and calculated structure factors of various reflections as a function of u was

TABLE I. Structural parameters of the $Zn_xNi_{1-x}Fe_2O_4$ system.

x	Lattice constant a_0 (Å)	u	T_N (°K)	T_{YK} (°K)	Cation distribution	$B_{R.T.}$ (10^{-16} cm²)	θ_D (°K)
0	8.325±0.008	0.2573±0.0003	(873)[a]	0	$(Fe^{3+})[Ni^{2+}Fe^{3+}]$	0.80	366
0.25	8.346±0.008	0.2561±0.0003	725	300	$(Zn_{0.25}^{2+}Fe_{0.75}^{3+})[Ni_{0.75}^{2+}Fe_{1.25}^{3+}]$	0.50	466
0.50	8.374±0.008	0.2573±0.0003	550	400	$(Zn_{0.50}^{2+}Fe_{0.50}^{3+})[Ni_{0.50}^{2+}Fe_{1.50}^{3+}]$	0.70	389
0.75	8.400±0.008	0.2598±0.0003	375	375	$(Zn_{0.75}^{2+}Fe_{0.25}^{3+})[Ni_{0.25}^{2+}Fe_{1.75}^{3+}]$	0.80	362

[a] C. Guillaud, J. Phys. Radium 12, 239 (1951).

[18] M. Sage and C. Guillaud, Compt. Rend. **230**, 1751 (1950).

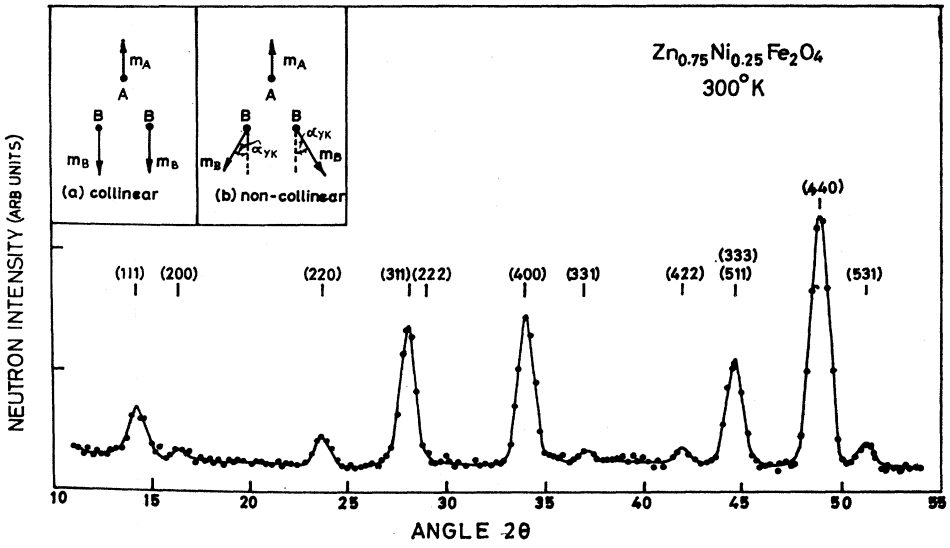

FIG. 2. Neutron-diffraction pattern of polycrystalline $Zn_{0.75}Ni_{0.25}Fe_2O_4$ at room temperature. The inset shows the schematic models considered: (a) is the collinear model and (b) is the noncollinear model of the Yafet-Kittel type. α_{YK} is the Yafet-Kittel angle.

employed to determine the u parameters. Figures 1(a)–1(c) show the evaluations for $x=0.75$, 0.50, and 0.25, respectively, using the high-temperature data. In the case of $NiFe_2O_4$, the oxygen parameter was precisely determined using the combination of ratios of the structure factors at room temperature of (311), (511), (333), and (440). Table I lists all the relevant structural parameters determined in the present study. The scattering amplitudes of Fe and Ni are so close to each other (0.96×10^{-12} and 1.03×10^{-12} cm, respectively) that the Fe and Ni distribution cannot be conclusively inferred from the nuclear scattering amplitudes alone. The cation distributions were, therefore, determined on the basis of the best agreement of the room-temperature intensities. The agreement of observed and calculated nuclear intensities for the high-temperature patterns is shown in Table II. The final effective scattering amplitudes for the A and B sites are also shown. From the values of b_A for the ferrites, it is immediately clear that all the zinc ions with their smaller scattering amplitudes of $b=0.59\times10^{-12}$ cm are on the A sites (because the b_B values lie between the scattering amplitudes of iron and nickel in all the cases). The analysis of the room-temperature intensities in all the cases again shows that the measured magnetic moments on the A sites ($4.87\mu_B$, $3.60\mu_B$, $2.30\mu_B$, and $1.10\mu_B$ for $x=0$, 0.25, 0.50, and 0.75, respectively) are much too large to have any nickel ions on the A sites. In fact, if spin-only moments are allowed for Fe^{3+} ions there can be no Ni^{2+} ions on the A sites. This conclusion is also borne out by recent measurements of Robertson and Pointon[19] of the perference energy of the Ni^{2+} ions for the B sites to be 0.80 ± 0.05 eV. They concluded that the maximum percentage of Ni^{2+} ions that can occupy the A sites is only about 1% even for samples quenched from near the melting point of the ferrite. Ferrimagnetic resonance measurements and effect of Ni^{2+} ions in the tetrahedral sites on the anisotropy constants and effective g factor also set a minimum degree of inversion.[20]

MAGNETIC STRUCTURES

The room-temperature patterns were used to deduce the magnetic structures. The calculations were mainly based on two models, illustrated in the inset of Fig. 2, namely, (a) a collinear arrangement and (b) a noncollinear arrangement of the Yafet-Kittel type. Spiral structures were not considered in view of the lack of evidence of any satellite reflections. In the YK model, a splitting of the B sublattice was assumed with the magnetic moments in the B_1 and B_2 sublattices equal in magnitude and each making an angle α_{YK} with the direction of the net magnetization at 0°K ($2\alpha_{YK}$ being

TABLE II. Comparison of observed and calculated nuclear intensities for $Zn_xNi_{1-x}Fe_2O_4$.

	$x=0.75$ $T=450$°K		$x=0.50$ $T=600$°K		$x=0.25$ $T=800$°K	
hkl	R.I. (obs)	R.I. (calc)	R.I. (obs)	R.I. (calc)	R.I. (obs)	R.I. (calc)
111	16.67	16.50	10.81	10.91	7.72	7.39
220	9.52	9.53	11.49	11.13	13.00	12.76
311	50.60	50.41	55.40	55.25	58.34	57.16
222	0.89	0.87	0.88	0.88	0.75	0.77
400	55.36	55.31	51.35	51.38	47.01	45.93
331	0.36	0.26	0.47	0.45	0.35	0.32
422	4.76	4.94	6.08	6.35	7.56	7.51
511} 333}	40.48	41.81	39.19	38.05	37.61	37.14
440	100.00	100.00	100.00	100.00	100.00	100.00
531	9.52	10.35	4.05	5.42	3.92	3.45
R		0.0065		0.0127		0.0133
$b_A(10^{-12}$ cm)		0.6825		0.7750		0.8675
$b_B(10^{-12}$ cm)		0.9688		0.9775		0.9863

[19] J. P. Robertson and A. J. Pointon, Solid State Commun. **4**, 257 (1966).

[20] A. J. Pointon and J. M. Robertson, Phil. Mag. **17**, 703 (1968).

TABLE III. Comparison of observed and calculated relative intensities at room temperature for $Zn_{0.75}Ni_{0.25}Fe_2O_4$.

hkl	I	II	III	IV	R.I. (obs)
111	29.45	20.75	28.48	22.69	21.54
200	0	0	16.01	4.03	3.85
220	9.43	9.73	9.73	9.73	10.00
311	51.64	49.06	52.68	49.97	51.54
222	5.97	1.88	1.88	1.88	2.00
400	56.57	54.90	54.90	54.90	55.72
331	2.31	0.98	2.16	1.28	1.30
422	4.91	4.98	7.58	5.14	5.15
511/333	41.86	41.52	42.13	41.67	41.54
440	100.00	100.00	100.00	100.00	100.00
531	8.28	7.92	8.28	8.01	8.00

Model	Magnetic moments (μ_B)				
	m_A	$m_{B\|\|A}$	$m_{B\perp A}$	m_B	α_{YK}
I	0.80	2.90	0	2.90	0
II	1.10	1.30	0	1.30	0
III	1.10	1.30	2.59	2.90	68°
IV	1.10	1.30	1.30	1.84	45°±2.5°

the angle between the moments on the B_1 and B_2 sites). This model is similar to that suggested by Niessen.[21] The resultant moment of the B sublattice is still collinear with, but antiparallel to, that of the A sublattice. The presence of a measurable (200) reflection in the pattern for $x=0.75$ offers striking support for the existence of a splitting in the B sublattice while the assumption of an unsplit A sublattice is justified by the agreement of the intensities of the (220) reflections (which depend only on the A-sublattice moment).

Following Hastings and Corliss[22] the magnetic-structure factors for an unmagnetized polycrystalline sample can be written as

$$\langle|M|^2\rangle_{hkl}=\tfrac{2}{3}|\mathcal{S}_A\langle p\mathbf{k}\rangle_A+\mathcal{S}_B\langle p\mathbf{k}\rangle_B|_{hkl}{}^2,$$

where $\mathcal{S}_A$ and $\mathcal{S}_B$ are the geometrical structure factors

$$\mathcal{S}_A=\sum_A \exp[2\pi i(hx_A+ky_A+lz_A)]$$

and

$$\mathcal{S}_B=\sum_B \exp[2\pi i(hx_B+hy_B+lz_B)].$$

The usual $q^2=\frac{2}{3}$ factor here corresponds to averaging the direction of the "structure-weighted" mean spin vector in the direction of the net moment, namely,

$$\mathcal{S}_A\langle p\mathbf{k}\rangle_A+\mathcal{S}_B\langle p\mathbf{k}\rangle_B,$$

where $\mathbf{k}$ is the direction of the net magnetization.

TABLE IV. Comparison of observed and calculated sublattice and net magnetic moments (Bohr magnetons) in $Zn_{0.75}Ni_{0.25}Fe_2O_4$ at various temperatures.

	Collinear			Observed[a] (YK)			
T (°K)	A	B	Net	A	B	Net	α_{YK}
0	1.25	9.32	8.07	1.25	4.64	3.39	60°
125	1.20	8.97	7.77	1.21	4.20	2.99	55°
300	0.78	5.86	5.08	1.10	2.60	1.50	45°
325	0.65	4.87	4.22	0.92	1.92	1.00	18°
365	0.28	2.12	1.84	0.70	0.68	−0.02	0

[a] The 0°K moments are from extrapolation of observed values.

[21] K. F. Niessen, Physica **19**, 1035 (1953).
[22] J. M. Hastings and L. M. Corliss, Phys. Rev. **90**, 1013 (1953).

$Zn_{0.75}Ni_{0.25}Fe_2O_4$

For zinc concentrations in the region of $x=0.75$ the net moment is very sensitive[1–5] to zinc content. The diffraction pattern for this ferrite is shown in Fig. 2. The most striking feature of the pattern is the existence of the (200) reflection, which is a manifestation of the canting of the B-site spins. The magnetic moments at various temperatures on the A and B sites were determined from the observed intensities. Table III shows the comparison of the observed and calculated relative intensities at room temperatures for this composition. The calculated intensities are according to four different

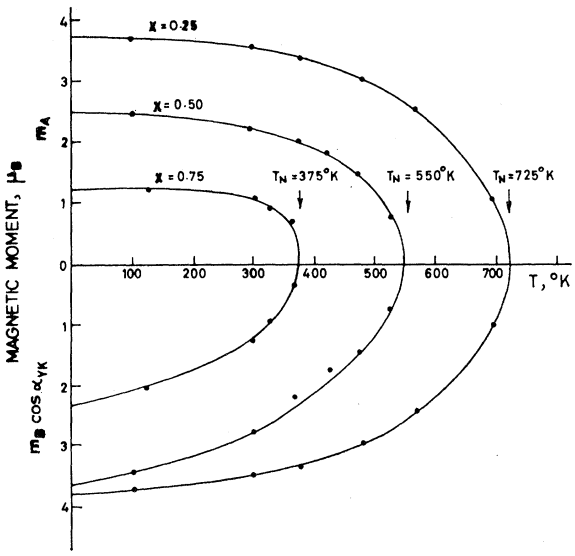

FIG. 3. A- and B-sublattice magnetizations for $x=0.25$, 0.50, and 0.75.

models. The corresponding sublattice moments are shown at the bottom of the table: Model I is a collinear model as in the inset (a) of Fig. 2 with the A- and B-site moments taken as the room-temperature values of the "spin-only" moments, assuming a simple Brillouin dependence. This model is clearly not possible as it does not yield the correct net moment. The moments can be adjusted as in model II to yield the correct net moment, choosing an m_A value to fit the (220) intensity and taking m_B as equal to $\frac{1}{2}(m_{net}+m_A)$, but this does not account for the (200) intensity. m_A, m_B, and m_{net} here represent the sublattice and net magnetic moments. [Any assumption of cation order on the B sites to explain the presence of (200) will affect all the nuclear intensities and no agreement is possible.] Model III

has the same A-site moment as model II but the B-site moment is canted with respect to the A-site moment to yield the correct net moment. This, however, yields too high a (200) intensity and the agreement with the other intensities is also not very good. Best agreement with (200) as well as other intensities is found for model IV, which is as shown in the inset (b) of Fig. 2 with m_A taken as 1.10 μ_B and $m_B=1.84\mu_B$ with the angle $\alpha_{YK}=45°\pm2.5°$. The agreement of the (200) intensity is seen to be quite reasonable. The (200) intensity was accurately estimated after carefully assessing the second-order contamination of the monochromatic beam which was found to be less than $\frac{1}{2}$ of 1%. Table IV shows the resultant magnetic moments on the A and B sites at various temperatures according to the YK arrangement. Also shown for comparison are the A- and B-site moments for a collinear arrangement, assuming a g factor for $Fe^{3+}=2$ and a g factor for $Ni^{2+}=2.3$ (Ref. 23) and a simple Brillouin dependence with temperature. From Fig. 3, which shows the observed temperature dependence of the sublattice magnetization extracted from the experimental intensities, it is obvious that the collinear model is not satisfactory. The data taken at 125°K are also best fitted with the YK model with $m_A=1.21\mu_B$ and $m_{B\text{II}A}=2.10\mu_B$, with $\alpha_{YK}=55°\pm2.5°$. At 0°K, the extrapolated value of $m_{B\text{II}A}$ is $2.32\mu_B$; the calculated B-site moment is $4.66\mu_B$ so that the YK angle at 0°K is found to be 60°.

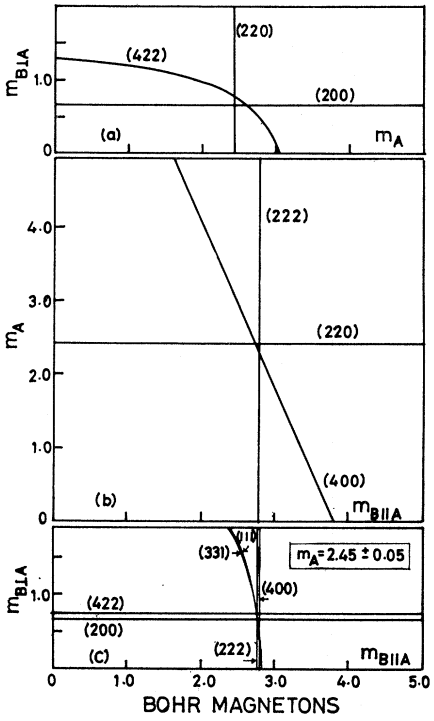

FIG. 4. Magnetic-moment plots for various magnetic-structure factors in $Zn_{0.5}Ni_{0.5}Fe_2O_4$ at room temperature.

TABLE V. Comparison of observed and calculated relative intensities at room temperature for $Zn_{0.5}Ni_{0.5}Fe_2O_4$.

hkl	R.I. (calc)	R.I. (obs)	WK (obs)[a]
111	31.08	29.55	27.83
200	0.90	1.00	...
220	12.12	12.50	13.08
311	50.64	50.00	56.25
222	5.67	5.63	5.53
400	51.41	51.14	57.84
331	3.92	3.41	2.85
422	6.72	6.82	6.87
511, 333	37.30	39.77	39.23
440	100.00	100.00	100.00
531	6.68	7.03	

[a] V. C. Wilson and J. S. Kasper, Phys. Rev. **95**, 1408 (1954).

$Zn_{0.5}Ni_{0.5}Fe_2O_4$

A previous neutron-diffraction study on the magnetic structure of this ferrite has been made by Wilson and Kasper (WK).[11] The magnetic ordering at room temperature was concluded by them to be of the Néel type with 60% of the Fe^{3+} ions on both sites antiparallel and all the Ni^{2+} ions randomly oriented. This ordering implies an A-site moment of $1.50\mu_B$ and a B-site moment of $2.25\mu_B$, leading to a net moment of $3.0\mu_B$. The absolute magnetic structure factors were extracted from the room-temperature intensities. In Fig. 4 are shown the magnetic-moment plots, namely, $m_{B\perp A}$ versus m_A, m_A versus $m_{B\text{II}A}$, and $m_{B\perp A}$ versus $m_{B\text{II}A}$ for the various magnetic-structure factors. These graphs yield the value of $m_A=2.45\mu_B$, $m_{B\text{II}A}=2.80\mu_B$, and $m_{B\text{II}A}=0.65\mu_B$ or $m_B=2.87\mu_B$ with $\alpha_{YK}=13°$, yielding a net moment of $3.25\mu_B$. The comparison of the observed and calculated intensities at room temperature based on these parameters is shown in Table V. The WK-observed room-temperature intensities are also shown for comparison. The temperature variation of the sublattice moments is shown in Fig. 3 and also in Table VI. The table shows the net magnetic moment of

TABLE VI. Comparison of observed and calculated sublattice and net magnetic moments (Bohr magnetons) in $Zn_{0.5}Ni_{0.5}Fe_2O_4$ at various temperatures.

	Collinear		Observed (YK)					
T (°K)	A	B	Net	A	B	Net[a]	Net[b]	α_{YK}
0	2.50	8.65	6.15	2.49	7.30	4.81	4.86	32°
100	2.48	8.57	6.09	2.48	7.06	4.58	4.60	25°
300	2.15	7.49	5.34	2.45	5.60	3.25	3.20	13°
375	1.89	6.65	4.76	1.99	4.40	2.41	2.53	5°
425	1.64	5.73	4.09	1.83	3.56	1.73	1.97	0
475	1.33	4.64	3.31	1.52	3.00	1.48	1.42	0
525	0.73	2.55	1.82	0.73	1.50	0.77	0.60	0

[a] Neutron-diffraction 0°K moments are from extrapolation of observed values.
[b] Saturation magnetization data from Ref. 2, p. 158.

[23] H. G. Beljers and D. Polder, Nature **165**, 800 (1950). See also *Handbook of Microwave Ferrite Materials*, edited by W. H. von Aulock (Academic Press Inc., New York, 1965).

the ferrite as deduced from the present measurements along with those from saturation magnetization measurements. Also listed for comparison are the net and sublattice moments for a collinear structure. It is seen that the agreement with the YK model is very good. The WK model would not lead to the correct sublattice or net moments at 0°K since, at this temperature, complete order among the moments should result in values given for the Néel configuration. The extrapolated 0°K moments are quite a bit lower. It can also be seen that as in the case of $x=0.75$ that α_{YK} is strongly temperature-dependent. It decreases with increasing temperature, going to zero at about 400°K. Beyond this temperature the magnetic structure is collinear, of the Néel type, up to the paramagnetic transition at $T_N=550$°K. The 100°K data yield values of $m_A=2.48\mu_B$ and $m_{B\|A}=3.53\mu_B$, leading to an $\alpha_{YK}=25°$. At 0°K, the extrapolated value of $m_{B\|A}=3.65\mu_B$ and the calculated B-site moment is $4.325\mu_B$, indicating a YK angle of 32°.

$Zn_{0.25}Ni_{0.75}Fe_2O_4$

For this composition, the net moment lies in the linear region of the curve of saturation magnetization versus x, so that a collinear ferrimagnetic arrangement may be considered likely. The room-temperature intensities do indeed lead to a collinear model with $m_A=3.60\mu_B$. These values were derived by a graphical examination of the magnetic structure factors of several reflections, as shown in Fig. 5. The intersections of the lines gives the best values of m_A and m_B. The agreement of the intensities is shown in Table VII. The pattern at 100°K, however, gave intensities which do not agree with the collinear model and a YK angle of $\alpha_{YK}=10°\pm2.5°$ has to be invoked to fit the data. At this temperature $m_A=3.72\mu_B$ and $m_{B\|A}=3.72\mu_B$ and $m_{B\perp A}=0.66\mu_B$ or $m_B=3.78\mu_B$. These yield an excellent agreement with the saturation magnetization measurement of the sample at room temperature. Figure 3 shows the temperature variation of the sublattice magnetization and Table VIII gives the values of the sublattice and net observed moments at various temperatures compared with those based on a Néel arrangement. In view of the small magnitude of the angles, the differences between the net moments in the two cases is not large but are still measurable. As in the two previous cases, the YK angle shows a strong temperature dependence going to zero at 300°K. The Néel region in this case is wide, persisting between 300 and 725°K (T_N). At 0°K, the extrapolated $m_{B\|A}=3.80\mu_B$ and the calculated B-site moment is $3.985\mu_B$, indicating a YK angle of 17.6°.

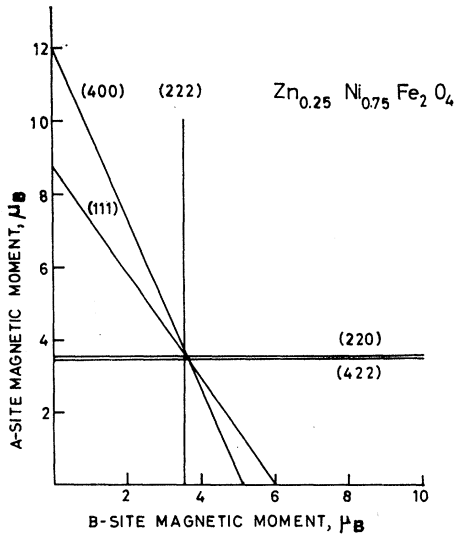

FIG. 5. Magnetic-moment plot for various magnetic-structure factors in $Zn_{0.25}Ni_{0.75}Fe_2O_4$ at room temperature.

TABLE VII. Comparison of the observed and calculated intensities at room temperature and 100°K for $Zn_{0.25}Ni_{0.75}Fe_2O_4$.

	$T=300$°K		$T=100$°K	
hkl	R.I. (calc)	R.I. (obs)	R.I. (calc)	R.I. (obs)
111	40.81	40.70	42.54	42.53
200			0.85	0.90
220	15.53	15.70	15.38	15.31
311	51.72	51.74	50.42	50.38
222	8.52	8.14	8.46	8.32
400	49.06	45.42	48.52	48.87
331	6.27	6.40	6.76	6.80
422	8.16	8.14	8.33	8.32
511, 333	36.96	37.21	36.74	37.05
440	100.00	100.00	100.00	100.00
531	5.73	5.81	5.98	6.14

$NiFe_2O_4$

The room-temperature intensities of $NiFe_2O_4$ were best fitted with a completely inverted collinear model with $m_A=4.87\mu_B$ and $2m_B=6.95\mu_B$, leading to a net moment of $2.08\mu_B$, which is in agreement with the observed magnetization results. The calculated intensities are shown in Table IX. The observed intensities of Hastings and Corliss[10] (HC) have been included for comparison. The intensities at 100°K were substantially the same as those at room temperature, indicating

TABLE VIII. Comparison of observed and calculated sublattice and net magnetic moments (Bohr magnetons) in $Zn_{0.25}Ni_{0.75}Fe_2O_4$ at various temperatures.

	Collinear			Observed[a] (YK)			
T (°K)	A	B	Net	A	B	Net	α_{YK}
0	3.75	7.97	4.22	3.75	7.60	3.85	17.6°
100	3.73	7.94	4.21	3.72	7.44	3.72	10°
300	3.50	7.50	4.00	3.60	7.00	3.40	0
380	3.30	7.03	3.73	3.39	6.69	3.30	0
480	2.90	6.26	3.36	3.03	5.93	2.90	0
570	2.40	5.21	2.81	2.52	4.90	2.38	0
700	1.09	2.40	1.31	1.07	2.02	0.95	0

[a] 0°K moments are from extrapolation of observed values.

TABLE IX. Comparison of calculated and observed relative neutron intensities at 300°K for $NiFe_2O_4$.

hkl	R.I. (calc)	R.I. (obs)	HC (obs)[a]
111	51.48	50.48	44.21
200	0	0	0
220	22.35	25.35	22.35
311	56.04	56.28	58.43
222	8.16	7.77	7.59
400	48.62	49.85	49.68
331	7.96	7.77	8.00
422	10.39	10.97	11.62
511, 333	40.30	40.75	39.57
440	100.00	100.00	100.00
531	5.72	5.83	6.70

[a] J. M. Hastings and L. M. Corliss, Rev. Mod. Phys. 25, 114 (1953).

almost complete saturation. The present analysis was made using the individual ion form factors (available from self-consistent Hartree-Fock calculations), where as the HC analysis used a composite form factor derived by them using the (111) and (444) intensities. Recently, Morel[24] has measured the sublattice magnetizations in $NiFe_2O_4$ using Mössbauer techniques. Using his data, the 0°K magnetic moment of the Ni^{2+} ion in the present sample was found to be $2.3\mu_B$ and that of the Fe^{3+} ion was found to be $5.0\mu_B$. The moment of nickel at 0°K which is greater than the spin-only value of $2\mu_B$ can be exactly accounted for using a g factor for the Ni^{2+} ion of 2.3, as given in Ref. 23.

SYSTEMATICS OF MAGNETIC PROPERTIES

The foregoing results clearly show the existence of a systematic behavior in the magnetic ordering of the Zn-Ni ferrites. The presence of a YK type of ordering at intermediate compositions has been established beyond doubt. The ordering scheme can be explained in the molecular-field approximation in terms of a three sublattice model involving a splitting of the B sublattice into B_1 and B_2 sublattices, and taking into account the interactions between and within all the sublattices. The present study has brought out the following systematics in the system

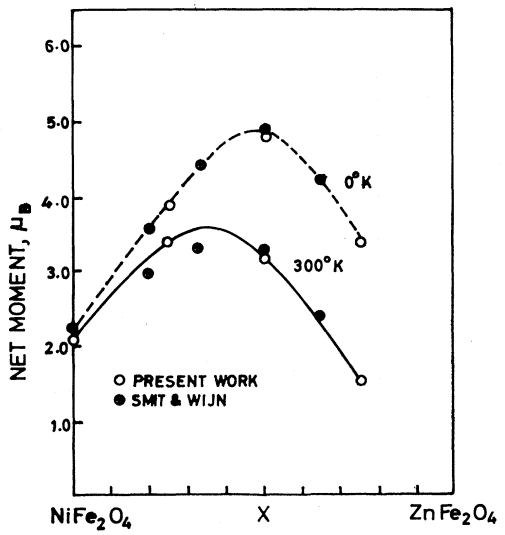

FIG. 6. Net magnetic moments at 0 and 300°K for the system $Zn_xNi_{1-x}Fe_2O_4$ as obtained from neutron diffraction. The saturation magnetization data from Smit and Wijn are included for comparison.

[24] J. P. Morel, J. Phys. Chem. Solids 28, 629 (1967).

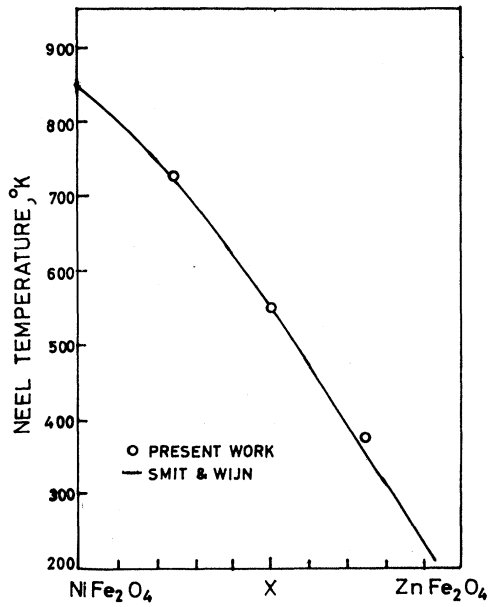

FIG. 7. Néel temperatures of the $Zn_xNi_{1-x}Fe_2O_4$ system. The full line is taken from Smit and Wijn.

The variation of the net ferric moment with composition at 300°K and at 0°K as derived from the present results is shown in Fig. 6 along with values from saturation magnetization measurements quoted in Smit and Wijn.[2] The agreement is seen to be quite good. The Yafet-Kittel angles readily account for this variation as shown earlier.

The Néel temperatures of the ferrites as a function of concentration of zinc are shown in Fig. 7, in which the full line was taken from Ref. 2. It is seen that there is a sharp decrease of Néel temperature for small additions of zinc. This is due to the decreasing number of A-B interactions resulting from the substitution of nickel by zinc. A quantitative expression for this variation would involve the various sublattice magnetizations in a complicated way.

The system shows the very interesting feature of two magnetic transitions: from a YK to a Néel configuration at a temperature T_{YK} and from the Néel arrangement to the paramagnetic region at the usual Néel temperature T_N. Figure 8 shows the temperature variations of the YK angle for the three intermediate compositions. Also shown for comparison in each case is the total intensity

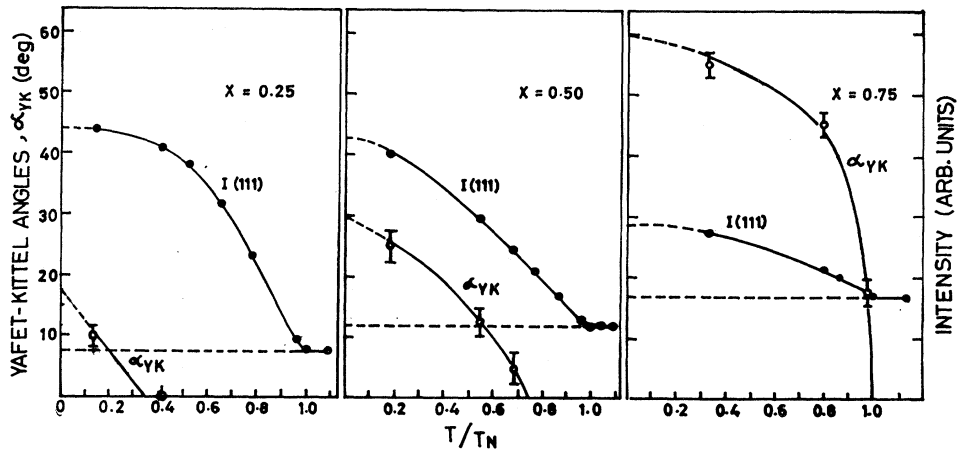

FIG. 8. Variation of the Yafet-Kittel angles with reduced temperature for $x=0.25$, 0.50, and 0.75. Shown also is the temperature dependence of the (111) intensity. The horizontal dashed lines indicate the level of nuclear intensity.

of the (111) reflection. (The broken horizontal line represents the nuclear intensity.) It is seen that, for $x=0.25$ and 0.50, the YK angle goes to zero well before the magnetic contribution to the (111) intensity vanishes. Lotgering[25] and Boucher *et al.*[26] have previously pointed out the occurrence of such transitions in the three sublattice ferrimagnets. Plumier[27] has observed similar transitions in his neutron-diffraction study of MnV_2O_4. In the present study, the transitions T_{YK} have been determined to be 300, 400, and 375°K for $x=0.25$, 0.50, and 0.75, respectively. A plot of T_{YK}/T_N is given in Fig. 9. It is seen that the temperature region of the Néel configuration decreases with increasing zinc content. This is probably due to the decrease in the number of Ni^{2+}-Ni^{2+} interactions in B sublattices. The curve extrapolates on the left nearly

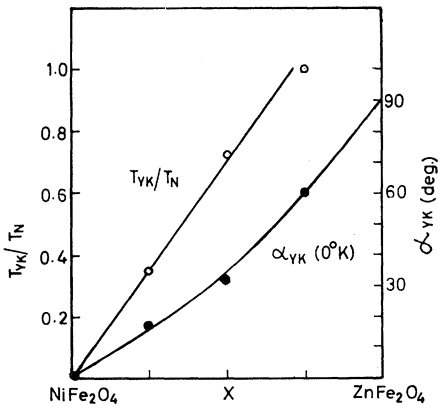

FIG. 9. Variation of the ratio T_{YK}/T_N and Yafet-Kittel angle at 0°K with composition.

to zero, indicating that $NiFe_2O_4$ is a Néel ferrimagnet at all temperatures. At $x=0.75$ the curve reaches the value of unity, showing that for and beyond this composition there is no Néel region.

The variation of the YK angle (extrapolated to 0°K) with concentration is of course the most striking observation in the present study. This is also shown in Fig. 9. A solid line drawn through the measured angles extrapolates to 90° for $ZnFe_2O_4$ indicating that it is a collinear antiferromagnet. It is possible to write an analytical expression describing the dependence of the YK angles on composition in the molecular field approximation. Using the noncollinear three sublattice ordering scheme shown in the inset (b) of Fig. 2, the following set of interactions can be defined: Let the interactions A(Fe)-A(Fe), A(Fe)-B_1(Ni), A(Fe)-B_1(Fe), A(Fe)-B_2(Ni), A(Fe)-B_2(Fe), B_1(Ni)-B_2(Ni), B_1(Fe)-B_2(Fe), B_1(Ni)-B_2(Fe), and B_1(Fe)-B_2(Ni) be represented by the molecular-field constants λ_{AA}, α, β, α, β, γ, δ, ϵ, and ϵ, respectively. The molecular fields acting on the various ions are given by

$$\begin{pmatrix} \mathbf{H}_A(\mathrm{Fe}) \\ \mathbf{H}_{B1}(\mathrm{Ni}) \\ \mathbf{H}_{B1}(\mathrm{Fe}) \\ \mathbf{H}_{B2}(\mathrm{Ni}) \\ \mathbf{H}_{B2}(\mathrm{Fe}) \end{pmatrix} = \begin{pmatrix} \lambda_{AA} & \alpha & \beta & \alpha & \beta \\ \alpha & \gamma & \epsilon & \gamma & \epsilon \\ \beta & \epsilon & \delta & \epsilon & \delta \\ \alpha & \gamma & \epsilon & \gamma & \epsilon \\ \beta & \epsilon & \delta & \epsilon & \delta \end{pmatrix} \begin{pmatrix} (1-x)\mathbf{m}_A(\mathrm{Fe}) \\ \tfrac{1}{2}(1-x)\mathbf{m}_{B1}(\mathrm{Ni}) \\ \tfrac{1}{2}(1+x)\mathbf{m}_{B1}(\mathrm{Fe}) \\ \tfrac{1}{2}(1-x)\mathbf{m}_{B2}(\mathrm{Ni}) \\ \tfrac{1}{2}(1+x)\mathbf{m}_{B2}(\mathrm{Fe}) \end{pmatrix},$$

where $\mathbf{H}_A$(Fe) is the molecular field acting on the Fe^{3+} ion on the A site due to all other ions, etc., and

$$|\mathbf{m}_A(\mathrm{Fe})| = |\mathbf{m}_{B1}(\mathrm{Fe})| = |\mathbf{m}_{B2}(\mathrm{Fe})| = 5\mu_B,$$
$$|\mathbf{m}_{B1}(\mathrm{Ni})| = |\mathbf{m}_{B2}(\mathrm{Ni})| = 2\mu_B,$$
$$\mathbf{m}_{B1}\cdot\mathbf{m}_A = -|\mathbf{m}_{B1}||\mathbf{m}_A|\cos\alpha_{YK},$$
$$\mathbf{m}_{B2}\cdot\mathbf{m}_A = -|\mathbf{m}_{B2}||\mathbf{m}_A|\cos\alpha_{YK},$$
$$\mathbf{m}_{B1}\cdot\mathbf{m}_{B2} = |\mathbf{m}_{B1}||\mathbf{m}_{B2}|\cos 2\alpha_{YK}.$$

The part of the interaction energy involving the YK

[25] F. K. Lotgering, Philips Res. Rept. **11**, 190 (1956).
[26] B. Boucher, R. Buhl, and M. Perrin, Compt. Rend. **263**, 785 (1966).
[27] R. Plumier, Compt. Rend. **255**, 2244 (1962); and in *Proceedings of the International Conference on Magnetism, Nottingham, 1964* (The Institute of Physics and The Physical Society, London, 1964), p. 295.

angles can be written as

$$E(\mathrm{YK})=[10(1-x)^2\alpha+25(1-x^2)\beta]\cos\alpha_{\mathrm{YK}} -\tfrac{1}{4}[4(1-x)^2\gamma+25(1+x)^2\delta+20(1-x^2)\epsilon]\cos 2\alpha_{\mathrm{YK}}.$$

The energy is minimum for (i) $\sin\alpha_{\mathrm{YK}}=0$, which corresponds to the Néel configuration, or for

$$\text{(ii)}\quad \cos\alpha_{\mathrm{YK}}=\frac{10(1-x)^2\alpha+25(1-x^2)\beta}{4(1-x)^2\gamma+25(1+x)^2\delta+20(1-x^2)\epsilon},$$

which represents the situation where the YK ordering is feasible. From the observed variation of the YK angles with concentration it is possible to evaluate the ratios of the molecular-field constants. However, any such evaluation depends sensitively on the accuracy of the extrapolation of the observed angles to 0°K, and the exact composition at which angles begin to develop. A small error in the value of the YK angles can lead to large variations in the field constants. Hence, no such constants have been extracted in the present case. However, the present results are consistent with the paramagnetic susceptibility data of Néel and Brochet[28] on Zn-Ni ferrites, which has been analyzed by Srivastava[29] using a three-sublattice model in the molecular-field approximation. The latter analysis used with the above expression for $\cos\alpha_{\mathrm{YK}}$ predicts angles of 0°, 0°, 40°, and 60° for $x=0$, 0.25, 0.50, and 0.75, respectively.

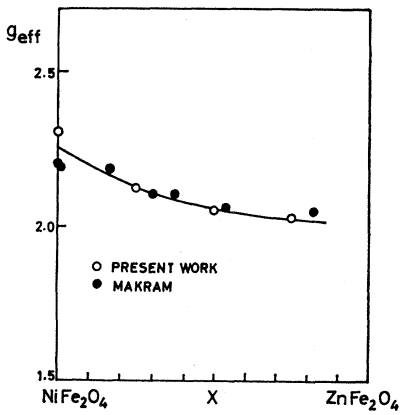

FIG. 10. Dependence of the g_{eff} with zinc content.

It is interesting to note that the present results can be used to evaluate the effective g values for these ferrites. If it is assumed that the value of g for the Ni^{2+} ion is 2.3 and that the Fe^{3+} ion has its orbital moment quenched throughout the system, the g_{eff} can be written as

$$g_{\mathrm{eff}}=\frac{g_{\mathrm{Ni}^{2+}}(1-x)+5(1+x)\cos\alpha_{\mathrm{YK}}-5(1-x)}{2(1-x)+5(1+x)\cos\alpha_{\mathrm{YK}}-5(1-x)} =\frac{(7.3+2.7x)\cos\alpha_{\mathrm{YK}}-5(1-x)}{(7.0+3x)\cos\alpha_{\mathrm{YK}}-5(1-x)}.$$

Figure 10 shows the g_{eff} values calculated from this expression substituting the observed angles at 0°K, along with g_{eff} values measured recently by Makram[30] by ferrimagnetic resonance. The agreement is seen to be quite satisfactory.

ACKNOWLEDGMENTS

The authors are indebted to Dr. P. K. Iyengar for his encouragement and keen interest in the work. They would like to thank Dr. C. Srinivasan for many useful discussions. Thanks are also due to C. S. Somanathan, B. S. Srinivasan, and M. R. L. N. Murthy for their valuable assistance in the experiments and to M. J. Patni for preparing the ferrite samples.

[28] L. Néel and P. Brochet, Compt. Rend. **230**, 280 (1950).
[29] C. M. Srivastava (unpublished).
[30] H. Makram, Czech. J. Phys. **B17**, 387 (1967).